JOURNAL OF CATALYSIS 66, 130–146 (1980)

Thermochemical Oscillations in Surface Reactions[1]

R. DAGONNIER, MARTINE DUMONT,[2] AND J. NUYTS

Faculté des Sciences, Université de l'Etat, B-7000 Mons, Belgium

Received July 19, 1979; revised May 26, 1980

The stability of a kinetic model for bimolecular surface reactions is analyzed. The model involves the surface temperature, as opposed to the ambient temperature, as a dynamical variable. Necessary conditions for surface reactions to exhibit self-sustained chemical oscillations are tentatively specified.

1. INTRODUCTION

Bimolecular catalytic surface reactions of the type

$$A(g) + \tfrac{1}{2}B_2(g) \xrightarrow[\text{surface}]{\text{catalytic}} AB(g) \qquad (1)$$

can exhibit instabilities like chemical oscillations. Such self-oscillations have been mainly observed in the heterogeneous catalytic *oxidation* of carbon monoxide (*1–6*), of hydrogen (*2, 7*), of ammonia (*8*), and of organic compounds (*9, 10*). Such surface reaction instabilities can be displayed within a kinetic model that involves an a priori variable *surface temperature T*. In a preliminary paper (*11*) we have reported numerical solutions of such model equations which reproduce qualitatively the chemical self-sustained oscillations, observed *at atmospheric pressure*, for the CO oxidation on SiO_2-supported Pt pellets (*3*).

The present objective is the geometrical and stability analysis of the model equations. Moreover, conditions for reaction (1) to exhibit self-sustained chemical oscillations will tentatively be specified. These conditions for oscillations depend not only on adjustable external parameters (ambient temperature T_a, partial pressures, catalyst setup, etc.) but also on intrinsic rate constants (frequency factors, activation energies) and enthalpies of reaction so that experimental checks of these conditions would provide a means for determining these internal parameters.

Further investigations on the oscillation characteristics (frequency, amplitude, form, etc.) in terms of the above-mentioned parameters should be performed for specific reactions (e.g. (*11*)). Practical interests should also be kept in mind such as increasing or improving the catalyst performance (reaction yield, specificity, etc.) in the oscillatory state as compared to those in the time-independent state.

Our model is based on the following assumptions:

(1) Gaseous reactants A and B_2 can competitively adsorb on active sites of the *same kind* (Σ) and react to produce molecules AB which leave the surface as soon as they are formed.

(2) The kinetics of the reaction are described in terms of the fractional coverages θ_A, θ_B and the surface temperature T, which are assumed to be *uniform* throughout the surface.

(3) All parameters governing heat and mass transfers, including the ambient temperature $T_a \neq T$), are kept constant.

(4) Any activation energy is coverage independent.

The assumptions require some comments. Assumption (1) implies that there is no buildup of the reaction product, i.e., that

[1] Work partly supported by the IRIS Program sponsored by the Belgian Ministry for Science Policy.

[2] Chargé de Recherches au Fonds National Belge de la Recherche Scientifique.

0021-9517/80/110130-17$02.00/0
Copyright © 1980 by Academic Press, Inc.
All rights of reproduction in any form reserved.

the AB molecules formed on the surface are weakly bound. Assumption (2) implies that the heat, "chemically" generated by the various reaction steps, is distributed randomly over the surface much faster than it is dissipated in the gas or lost in the catalyst support. High-pressure experiments performed on small pellets of a metallic catalyst settled on insulating supports should satisfy assumption (2) (*3, 6*). By assumption (3) we consider the experimental conditions as clear-cut boundary conditions. Note that in the oscillating heterogeneous catalytic oxidations mentioned above the oscillation characteristics barely depend on the flow rate. All these results show that these self-oscillations are not caused by mass transfer processes. Assumption (4) is made for mathematical simplicity. This rather crude assumption can be accepted in this preliminary analysis. Indeed, the actual oscillating heterogeneous catalytic oxidations (*1–10*) have two main features in common:

(i) They involve a competitive coadsorption of two chemical reactants sharply differing in their redox (electron donor–acceptor) properties.

(ii) The surface remains almost entirely covered, the experiments being done at high pressure ($p_{tot} \approx p_{atm}$) (*12*). Therefore activation energies depending on *specific* coverages could make the model more realistic. Unfortunately experimental work in this direction is still lacking although theoretical investigations on *isothermal* oscillating surface reactions involving coverage-dependent activation energies are making progress (*13*). Further work involving coverage-dependent activation energies within our model is underway.

The paper is organized as follows.

In Section 2 we give a general formulation of the model in terms of the kinetic steps for reaction (1). It results in an autonomous system of three *nonlinear* differential equations in the variables $\theta_A(t)$, $\theta_B(t)$, and $T(t)$.

In Section 3 we gather the mathematical tools which are used in the linearized stability analysis of the model equations and we classify the steady-state solutions. The allowed physical cases and their connections are reported in Tables 2–4. These tables are used repeatedly.

In Sections 4 and 5 we analyze two limiting situations described by the model; namely, the "Langmuir–Hinshelwood" and the "Eley–Rideal" cases, respectively.

In Section 6 we use the results of the two preceding sections to investigate geometrically the general two-reaction-path model and to specify general conditions for self-sustained thermochemical oscillations in surface reactions.

2. THE MODEL

The *three dynamical variables* of the problem are the fractional coverages

$$X = \theta_A, \qquad Y = \theta_B \tag{2}$$

with

$$X + Y \leq 1, \qquad 0 < (X, Y) \tag{3}$$

and the *putative* surface temperature T (i.e., the temperature of the first few layers of the catalyst):

$$T_a \leq T < \infty. \tag{4}$$

T is introduced in the kinetic coefficients A, B, C, etc. in the usual way:

$$A = A' \exp(-A''/T). \tag{5}$$

The frequency factors A' (sec^{-1}) and the activation energies A'' (deg.) are constant (see assumptions (3) and (4)).

The time evolution of the adsorbate is described by a trajectory $\{X(t), Y(t), T(t)\}$ in the prismatic phase space defined by Eqs. (3) and (4) (e.g., see Fig. 1A).

The kinetic scheme we adopt for reaction (1) consists of the steps listed in Table 1. Let us comment on these steps one by one according to their order in Table 1.

(1) Step 1 describes the *molecular* adsorption of reactant A on sites Σ with a

TABLE 1

Classification of the Steps (and Their Parameters) Involved in the Kinetic Scheme

Step No.	Step	Frequency factor (sec^{-1})	Activation energy	Enthalpy factor	Rate[a]
1	$A(g) + \Sigma \xrightarrow{B_1} A(s)$	B_1'	B_1''	β_1	$B_1(1 - X - Y)$
2a	$B_2(g) + 2\Sigma \xrightarrow{B_2/2} 2B(s)$	$B_2'/2$	B_2''	β_2 (per site)	$n = 1, 2$ $B_2(1 - X - Y)^n$
2b	$B(g) + \Sigma \xrightarrow{B_2} B(s)$	B_1'	B_2''	β_2	$n = 1$
3	$A(s) + B(s) \xrightarrow{C} AB(g)$	C'	C''	γ	$-CXY$
4	$A(g) + B(s) \xrightarrow{A_2} AB(g)$	A_2'	A_2''	α_2	$-A_2Y$
5	$A(s) \xrightarrow{A_1} A(g) + \Sigma$	A_1'	A_1''	α_1	$-A_1X$

[a] The corresponding rates taken into account in the general kinetic system, Eqs. (14a)–(14c).

frequency factor (*14–16*)

$$B_1' = \sigma_A p_A (2\pi m_A k T_a)^{-1/2} N_s^{-1}, \qquad (6)$$

where σ_A, p_A, T_a, and N_s represent respectively the sticking coefficient of gas A, its partial pressure, the ambient temperature, and the number of active sites Σ per square centimeter. As this adsorption is molecular it will be assumed below that it is almost *unactivated*, i.e.,

$$B_1'' \approx 0. \qquad (7)$$

(2) Step 2 represents the *activated* ($B_2'' \neq 0$) *dissociative* adsorption of reactant B_2 on sites Σ with a preexponential factor B_2' analogous to B_1', Eq. (6). This adsorption

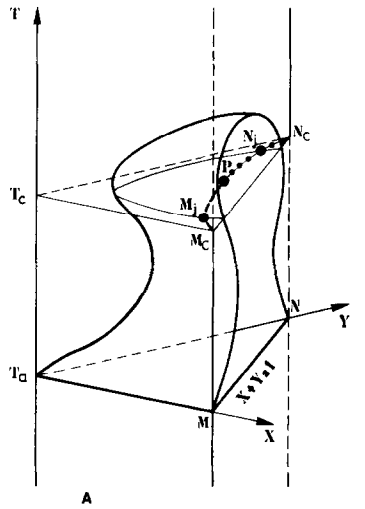

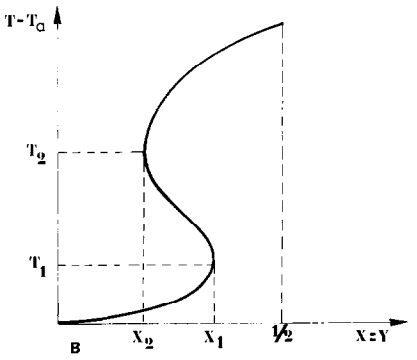

FIG. 1. (A) Representation in the physical prismatic phase space of the L–H steady-state lines in the case $n = 1$. The solid (dashed) lines represent stable (unstable) adsorbates. The dotted half-hyperbola in the plane at T_c corresponds to stable or unstable steady states (e.g., N_j). The surface (like a cowl) represents the L–H heat surface (see Eq. (22) where $A_2 = 0$). The steady-state points M_j and N_j are defined in Eqs. (38a) and (38b). (B) Intersection of the L–H heat surface with the plane $X = Y$. At the points (X_1, T_1) and (X_2, T_2) the derivative of X with respect to T vanishes; one has always $\frac{1}{2} > X_1 > X_2 > 0$ and, if $T_a \ll C''$, $T_1 - T_a \approx T_a^2/C''$ and $T_2 - T_a \approx C''$.

step 2 will be described by the coverage function

$$f_{\text{cov.}}(\text{B}) = (1 - X - Y)^n, \qquad n = 1 \text{ or } n = 2. \quad (8)$$

(i) $n = 1$: By using a linear coverage function either we picture the gas B_2 as made of *fictitious* molecules B (step 2a) *or* we refer simply to the reaction

$$\text{A(g)} + \text{B(g)} \xrightarrow[\text{surface}]{\text{catalytic}} \text{AB(g)}, \quad (9)$$

i.e., when both adsorptions are nondissociative, one of them at least being nevertheless activated (step 2b).

(ii) $n = 2$: The adsorption of B_2 is explicitly considered as dissociative (step 2a).

As, for a dissociative adsorption, no precise experimental fact supports the case $n = 2$ (*17*) and as more elaborated coverage functions involving the number z of nearest-neighbor sites Σ, e.g. (*14*),

$$f_{\text{cov.}}(\text{B}) = z(1 - X - Y)^2/(z - X - Y), \quad (10)$$

lead to an effective exponent lying between 1 and 2, we limit ourselves to the cases $n = 1$ and $n = 2$.

(3) Step 3 describes the *activated* ($C'' \neq 0$) Langmuir–Hinshelwood (L–H) surface reaction mechanism.

(4) Step 4 is the Eley–Rideal (E–R) reaction mechanism describing the pickup of the adsorbed atomic species B(s) by the gaseous molecule A(g). In a simple collisional model (see Eq. (6)) one has

$$A_2' = B_1'\sigma_{\text{E-R}}/\sigma_{\text{A}}, \quad (11)$$

where $\sigma_{\text{E-R}}$ stands for the "cross section" of this mechanism. We formally consider the E–R mechanism as almost *unactivated*, i.e.,

$$A_2'' \approx 0. \quad (12)$$

The "reciprocal" E–R mechanism is neglected,

$$\text{A(s)} + \text{B}_2\text{(g)} \not\rightarrow \text{AB(g)} + \text{B(s)},$$

but could easily be taken into account.

(5) Step 5 describes the activated desorption of molecules A (*14*):

$$A'' \neq 0, \qquad A' \approx 10^{13} \text{ sec}^{-1}. \quad (13)$$

The *associative* desorption of B, being generally highly activated, is neglected,

$$2\text{B(s)} \not\rightarrow \text{B}_2\text{(g)} + 2\Sigma.$$

However, if reaction (9) is taken into consideration, the reverse of step 2b (see Table 1) could be taken into account again.

The kinetic equations for this *two*-reaction-path model are

$$\frac{dX}{dt} = f_X(X, Y, T) \equiv -A_1X + B_1(1 - X - Y) - CXY, \quad (14a)$$

$$\frac{dY}{dt} = f_Y(X, Y, T) \equiv -A_2Y + B_2(1 - X - Y)^n - CXY, \quad (14b)$$

$$\frac{dT}{dt} = f_T(X, Y, T) \equiv -A_T(T - T_a) + \alpha_1A_1X + \alpha_2A_2Y + \beta_1B_1(1 - X - Y) + \beta_2B_2(1 - X - Y)^n + \gamma CXY. \quad (14c)$$

The production rate v (in molecules cm^{-2} sec^{-1}) is given by

$$v = N_s(A_2Y + CXY). \quad (15)$$

Equation (14c) describes the time evolution of the surface temperature T. The coefficients α, β, γ are proportional (through appropriate conversion factors (*11*)) to the enthalpies (heats) supplied or withdrawn by the various reaction steps. It is important to note that, according to our notation (see Table 1), β_2 represents the energy *per site* supplied by the dissociative adsorption of molecule B_2. The linear term $-A_T(T - T_a)$ describes the heat dissipation into the gas and through the catalyst toward its support, both gas and support being maintained at T_a (*18*). Roughly speaking, if we assume that the main contribution to the rate of relaxation of T to T_a is due to the

metallic catalyst, we should have

$$A_T \sim \frac{\kappa}{C_M \rho} \times \text{geometric factor},$$

where κ, C_M, and ρ are respectively the thermal conductivity, the specific heat, and the density of the catalyst.

As a *general prescription* we will consider that reaction (1) occurs in such a range of pressure and temperature that the catalyst surface remains almost entirely covered (*12*), i.e., under the condition

$$(B_1, B_2) > (C, A_1, A_2, A_T) > 0. \quad (16)$$

Moreover, according to the steps reported in Table 1 we will also use the following inequalities:

$$A_1'' > C'' > B_2'' > (A_2'', B_1'') \approx 0, \quad (17)$$

$$\beta_2 > (\beta_1, \alpha_2, \gamma) > 0, \qquad \alpha_1 \approx -\beta_1. \quad (18)$$

The only *formal* restriction used here is given by Eq. (12). The quasi-equality $\alpha_1 \approx -\beta_1$ is implied by the fact that, in the absence of reactant B, the model reproduces the *equilibrium* Langmuir isotherm for gas A (*14*):

$$X_L = B_1/(A_1 + B_1), \qquad T = T_a. \quad (19)$$

It should be added that a linear (or logarithmic) coverage dependence of the adsorption energy of A leads (in the absence of B) to a Tempkin (or Freundlich) isotherm (*14*) with $\alpha_1 = -\beta_1$. Finally it must be emphasized that Eq. (16) is the main condition used below while inequalities (17) and (18) will only be used under specification.

3. STABILITY ANALYSIS (IN GENERAL)

The steady states $\{X_0, Y_0, T_0\}$ of Eqs. (14a)–(14c) may be visualized in the phase space (see Eqs. (3) and (4) as the intersection points of the *steady-state lines* $\{X_0(T), Y_0(T)\}$, solutions of

$$f_X(X_0, Y_0, T) = 0, \quad (20a)$$

$$f_Y(X_0, Y_0, T) = 0, \quad (20b)$$

with the *heat surface*

$$f_T(X, Y, T) = 0. \quad (21)$$

In the vicinity of the steady-state points the heat surface equation (21) has approximately the following form ($\alpha_1 \approx -\beta_1$):

$$-(T - T_a) + LA_2Y + RCXY = 0, \quad (22)$$

where the factors L and R (in deg · sec) are positive constants measuring the heat available at the surface:

$$L = (\alpha_2 + \beta_2)/A_T, \quad (23a)$$

$$R = (\beta_1 + \beta_2 + \gamma)/A_T. \quad (23b)$$

To perform the linearized stability analysis of the steady states $\{X_0, Y_0, T_0\}$ one needs the eigenvalues of the 3×3 *Jacobian matrix* (*19*):

$$A = (A_{ij}) = (\partial f_i/\partial X_j)_{\{X_0, Y_0, T_0\}}, \qquad (i, j = X, Y, T), \quad (24)$$

where the f_i's are the r.h.s. of Eqs. (14a)–(14c). We thus have to solve the third-order characteristic equation

$$\lambda^3 - S_1\lambda^2 + S_2\lambda - S_3 = 0, \quad (25)$$

where S_i ($i = 1, 2, 3$) denotes the sum of all principal minors of A of order i. The various cases which can occur may be associated with regions in the S_i space in which we consequently investigate the stability of the steady states (*20*).

Using the matrix elements A_{ij}, Eq. (24), *under condition* (16) we obtain the following inequalities for the S_i's:

$$S_1 < 0, \ |S_2| \ll S_1^2, \ |S_3| \ll |S_1|^3. \quad (26)$$

All of the possible cases are classified in Table 2 using two auxiliary entries E and D related to the S_i's as follows (*20*):

$$E = S_3 - S_1S_2, \quad (27)$$

while, according to inequalities (26),

$$D \approx \tfrac{1}{27}S_1^2(S_1S_3 - \tfrac{1}{4}S_2^2). \quad (28)$$

The sign of E and D may be easily specified *when S_2 is different from zero*, as in this

TABLE 2

Classification of the Eigenvalues (λ_1, λ_2, λ_3) of Eq. (25) in the Physical $S_1 < 0$ and Nonpathological Cases[a]

				$S_3 > 0$	$S_3 < 0$
$S_1 < 0$	$S_2 > 0$	$D < 0$	$E > 0$	**1** $0 < \lambda_1 < \frac{\lambda_2\lambda_3}{\lvert\lambda_2\rvert + \lvert\lambda_3\rvert}$, $\lambda_2 < 0$, $\lambda_3 < 0$	**5** $\lambda_1 < 0$, $\lambda_2 < 0$, $\lambda_3 < 0$
		$D > 0$	$E > 0$	**2** $0 < \lambda_1 < 2\lvert\lambda_R\rvert$, $\lambda_R < 0$, $(2\lambda_1 - \lvert\lambda_R\rvert)\lvert\lambda_R\rvert < \lambda_I^2$	**6a** $\lambda_1 < 0$, $\lambda_R < 0$
			$E < 0$		**6b** $\lambda_1 < 0$, $\lambda_R > 0$, $2\lambda_R < \lvert\lambda_1\rvert < \frac{\lambda_R^2 + \lambda_I^2}{2\lambda_R}$, $3\lambda_R^2 < \lambda_I^2$
	$S_2 < 0$	$D < 0$	$E > 0$	**3a** $\frac{\lambda_2\lambda_3}{\lvert\lambda_2\rvert + \lvert\lambda_3\rvert} < \lambda_1 < \lvert\lambda_2\rvert$ or $\lvert\lambda_3\rvert < \lambda_1 < \lvert\lambda_2\rvert + \lvert\lambda_3\rvert$, $\lambda_3 < \lambda_2 < 0$	
			$E < 0$	**3b** $\lvert\lambda_2\rvert < \lambda_1 < \lvert\lambda_3\rvert$, $\lambda_3 < \lambda_2 < 0$	**7** $\lambda_1 < 0$, $\lambda_2 > 0$, $\lambda_3 > 0$, $\lambda_2 + \lambda_3 < \lvert\lambda_1\rvert$
		$D > 0$	$E > 0$	**4** $\frac{\lvert\lambda_R\rvert}{2} < \lambda_1 < 2\lvert\lambda_R\rvert$, $\lambda_R < 0$, $0 < \lambda_I^2 < (2\lambda_1 - \lvert\lambda_R\rvert)\lvert\lambda_R\rvert$	
			$E < 0$		**8** $\lambda_1 < 0$, $\lambda_R > 0$, $\frac{\lambda_R^2 + \lambda_I^2}{2\lambda_R} < \lvert\lambda_1\rvert$, $2\lambda_R < \lvert\lambda_1\rvert$

[a] When two eigenvalues are complex conjugate ($D > 0$) they are denoted $\lambda_2 = \lambda_R + \lambda_I = \lambda_3^*$. The arrows show the direct passages from one case to another.

case we have

$$|S_1S_3| < S_2^2, \qquad |S_3| < |S_1S_2|. \quad (29)$$

We classify in Table 2 the eigenvalues (λ_1, λ_2, λ_3) of Eq. (25) for the physical situation: $S_1 < 0$. In this classification we exclude the *pathological* cases that correspond to a zero value of one (or more) of the entries S_i, D, E of Table 2. Indeed, these pathological cases imply such precise relations between

TABLE 3

Classification of Cases of Table 2 Obtainable by Allowing *One* Given Parameter P to Vary Continuously So That P Can Reach a Value P_2 for Which $S_2(P_2) = 0$

	$S_2(P)$	$\geqslant 0$	>0	<0	$\leqslant 0$
	$D(P)$		<0	<0	<0
$S_3(P_2) > 0$					
	$E(P)$		>0	>0	<0
	Case		**1**	**3a**	**3b**
	$D(P)$	<0	>0	>0	<0
	$E(P)$	>0	>0 <0	<0	<0
$S_3(P_2) < 0$					
	Case	**5**	**6a** **6b**	**8**	**7**

the parameters involved in the problem that they are unlikely.

Moreover, we report in Tables 3 and 4 the situations that can be obtained by allowing *one given parameter*, say **P**, to vary continuously and reach values $\mathbf{P}_i$ ($i = 2, 3$) such that

$$S_i(\mathbf{P}_i) = 0 \qquad (i = 2, 3). \tag{30}$$

For physical reasons we disregard the direct *passages* from one case of Table 2 to another, for which *more than one* entry changes its sign. For instance, we consider the direct passage from case 5 to case 7 as forbidden; according to Table 3, this passage can only occur by following the sequence

$$\mathbf{5} \rightarrow \mathbf{6a} \rightarrow \mathbf{6b} \rightarrow \mathbf{8} \rightarrow \mathbf{7} \tag{31}$$

TABLE 4

Classification of Cases of Table 2 Obtainable by Allowing *One* Given Parameter P to Vary Continuously So That P Can Reach a Value P_3 for Which $S_3(P_3) = 0$

	$S_3(P)$	>0	<0
	$D(P)$	<0	<0
$S_2(P_3) > 0$	$E(P)$	>0	>0
	Case	**1**	**5**
	$D(P)$	<0	<0
$S_2(P_3) < 0$	$E(P)$	<0	<0
	Case	**3b**	**7**

The sign of S_i, D, and E gives us *local* conditions for the existence of instabilities (see Table 2). It should be emphasized that cases **6b** and **8** of Table 1 (i.e., "saddle spiral with unstable plane focus" (*20*)) correspond to *limit cycles* as the boundaries of the physically allowed phase space are *repulsive* for the solution $\{X(t), Y(t), T(t)\}$. It should also be noticed that the comparisons between Tables 3 and 4 and Table 2 show that cases **2** and **4** are *"isolated"* as we estimate the equality

$$\mathbf{P}_2 = \mathbf{P}_3$$

to be unlikely (see Eq. (30)).

We shall use Tables 2–4 to analyze the stability of a few limiting situations. Some of these situations, which involve *only one* reaction path, could be applied to particular surface reactions. We shall consider separately the cases $n = 1$ and $n = 2$ (see Eq. (8)). The following analysis of the one-reaction-path situations (see Sections 4 and 5) leads to oscillation (and/or stability) conditions that could be experimentally checked. Some surface reactions among those which exhibit self-oscillations (e.g. (*1–10*)) could provide us with such experimental tests for the model.

The results we shall obtain using the surface temperature as a variable could easily be compared with their corresponding *isothermal* version, i.e., when

$$T = T_a. \tag{32}$$

In this traditional version, any heat equation like Eq. (14c) is disregarded. The stability analysis is *two-dimensional* and concerns the intersection points $\{X_0(T_a), Y_0(T_a)\}$ of the steady-state lines ((20a), (20b)) with the plane (32) inside the phase space triangle, Eq. (3). We will not draw this comparison as such a two-variable model with uni- or bimolecular reaction steps *and* activation energies coverage independent cannot lead to limit cycles (*13, 21*).

4. "LANGMUIR-HINSHELWOOD" CASE

In this case both steps 4 and 5 (see Table 1) are neglected, i.e.,

$$A_1 = A_2 = 0. \tag{33}$$

Equations (14a)–(14c) then lead to the *pure* steady-state adsorbates:

$$M \equiv (X_0 = 1,\ Y_0 = 0,\ T_0 = T_a),$$
$$N \equiv (X_0 = 0,\ Y_0 = 1,\ T_0 = T_a), \tag{34}$$

and to *mixed* steady-state adsorbates $\{X_0, Y_0, T_0 > T_a\}$ that verify the following equations:

$$X_0 + Y_0 = 1 - (T_0 - T_a)/RB_1, \tag{35a}$$
$$X_0 Y_0 = (T_0 - T_a)/RC, \tag{35b}$$
$$B_1{}^n = B_2[(T_0 - T_a)/R]^{n-1}, \tag{35c}$$

where B_1, B_2, and C are evaluated at T_0 solution of Eq. (35c) and R is defined by Eq. (23b).

A. Stability Analysis of the L–H Adsorbates: Case n = 1

If $n = 1$ (see Eq. (8)), *mixed* L–H steady-state adsorbates are *only* obtained if T_0 is equal to the *critical* temperature T_c defined by Eq. (35c):

$$B_1(T_c) = B_2(T_c) \equiv B_c, \tag{36}$$

i.e.,

$$T_c = (B_2'' - B_1'')/\ln(B_2'/B_1'). \tag{37a}$$

Owing to the form of the B's (see Eq. (6)), T_c depends crucially on the ratio of the assumed partial pressures, i.e., with $B_1'' \approx 0$,

$$T_c = B_2''/\ln(p_B/p_A) + \text{constant}. \tag{37b}$$

These *mixed* L–H steady-state adsorbates correspond to a *pair* of *symmetric* points (see Fig. 1A):

$$M_j \equiv [X_c = \bar{X}_c(1 + \delta),\ Y_c = \bar{X}_c(1 - \delta),\ T_0 = T_c], \tag{38a}$$
$$N_j \equiv [X_c = \bar{X}_c(1 - \delta),\ Y_c = \bar{X}_c(1 + \delta),\ T_0 = T_c], \tag{38b}$$

where

$$\bar{X}_c = \tfrac{1}{2}[1 - (T_c - T_a)/RB_c] \tag{39}$$

and δ is the positive square root of

$$\delta^2 = 1 - 4B_c{}^2(T_c - T_a)/RC_c[B_c - (T_c - T_a)/R]^2 \tag{40}$$

with B_c given by Eq. (36) and $C_c \equiv C(T = T_c)$. For a particular value T_p of the *ambient* temperature T_a, δ is equal to zero and the points M_j and N_j coincide at point $P \equiv (X_p, Y_p, T_c)$ (see Fig. 1A) with

$$X_p \equiv Y_p = B_c[(1 + C_c/B_c)^{1/2} - 1]/C_c < \tfrac{1}{2} \tag{41}$$

and

$$T_p = T_c - RB_c(1 - 2X_p). \tag{42}$$

Therefore, if $n = 1$, mixed L–H steady-state adsorbates $\{X_c, Y_c, T_c\}$ can occur only for T_a in the range

$$T_p \leq T_a < T_c. \tag{43}$$

For the *pure* L–H adsorbates (34) the Jacobian matrix A (24) has the three following eigenvalues:

$$\lambda_{1,2} = -\tfrac{1}{2}\{B_1 + B_2 + C) \pm [(B_1 + B_2 + C)^2 - 4(B_1 - B_2)C(X_0 - Y_0)]^{1/2}\},$$
$$\lambda_3 = -A_T. \tag{44}$$

Therefore, as $B_2'' > B_1'' \approx 0$ (see Eq. (17)),

$$B_1 > B_2 \quad \text{for } T < T_c, \tag{44a}$$
$$B_1 < B_2 \quad \text{for } T > T_c, \tag{44b}$$

the point M is stable (unstable) if $T_0 = T_a < T_c$ (if $T_0 = T_a > T_c$) while, on the contrary, the point N is stable (unstable) if $T_0 = T_a > T_c$ (if $T_0 = T_a < T_c$) (see Fig. 1A). When $T_a = T_0 \equiv T_c$, the Jacobian matrix (24) is singular, i.e.,

$$S_1 < 0,\ S_2 > 0,\ S_3 = 0 \tag{45a}$$

and

$$\lambda_1 = -(2B_c + C_c),\quad \lambda_2 = 0,\ \lambda_3 = -A_T. \tag{45b}$$

The stability characteristics of the corresponding steady-state adsorbates (see Fig. 1A)

$$M_c \equiv (X_c = 1,\ Y_c = 0,\ T_0 = T_c),$$
$$N_c \equiv (X_c = 0,\ Y_c = 1,\ T_0 = T_c) \quad (46)$$

can be obtained *by continuity* from the stability analysis of the steady states M_j, N_j (see after Eq. (53) below). In the limit

$$T_a \overset{<}{\rightarrow} T_0 = T_c, \quad (47)$$

M_c is unstable (case 1 in Table 2) while N_c is stable (case 5) and the surface will be ultimately entirely covered with reactant B.

For the *mixed* L–H adsorbates (see Eqs. (38a), (38b)) occurring when T_a lies in the range (43), the S_i's take the following forms:

$$S_1 = -2(B_c + C_c\bar{X}_c) - A_T[1 - K(T_c - T_a)/T_c^2], \quad (48a)$$

$$S_2 = 2(B_c + C_c\bar{X}_c)A_T[1 - K(T_c - T_a)/T_c^2] - \{(2C'' - B_1'' - B_2'')[(\beta_1 + \beta_2)B_c - \gamma C_c\bar{X}_c] \pm (B_2'' - B_1'')\gamma C_c\bar{X}_c\delta\}(T_c - T_a)/RT_c^2, \quad (48b)$$

$$S_3 = \pm 2A_T B_c C_c \bar{X}_c \delta(B_2'' - B_1'')(T_c - T_a)/T_c^2, \quad (48c)$$

where the upper (lower) sign refers to M_j (N_j) (see Eqs. (38a), (38b)). According to inequalities (17) we have

$$0 \lesssim K = (\beta_1 B_1'' + \beta_2 B_2'' + \gamma C'')/(\beta_1 + \beta_2 + \gamma) < C''. \quad (49)$$

It is clear from the expressions ((48a)–(48c)) of the S_i's that the stability characteristics of points M_j and N_j should depend on the value of the *free parameter*

$$\Delta T = T_c - T_a > 0. \quad (50)$$

Considering a given reaction (1) one can vary this parameter ΔT by fixing T_a and varying T_c (i.e., by varying essentially the partial pressure ratio p_A/p_B, see Eq. (37b)) or, inversely, by fixing T_c and varying T_a. Let us discuss the stability of steady-state points M_j and N_j, Eqs. (38a), (38b), by choosing T_a as the free parameter P used in Tables 3 and 4 of Section 3.

Under conditions (16)–(18), Eqs. (48a)–(48c) show us that:

(i) S_1 remains negative for any physically acceptable value of T_a lower than T_c.

(ii) When T_a departs from T_c, S_3 keeps its sign but vanishes identically when $T_a = T_p$ (i.e., $\delta = 0$, see Eq. (42)):

$$S_3(T_a = T_p) = 0. \quad (51)$$

(iii) S_2, being positive when $T_a \overset{<}{\rightarrow} T_c$, becomes negative when T_a reaches a certain value T_2:

$$S_2(T_a = T_2)\ 0 \quad (52)$$

with T_2 slighty closer to T_c for M_j than for N_j.

Going back to Table 4 and using Eqs. (51) and (52) one readily concludes that if

$$T_P > T_2, \quad (53)$$

M_j is *unstable* (case **1** of Table 2) and N_j is *stable* (case **5**) for every value of T_a in the range (43). If inequality (53) is *reversed*, Table 3 shows us that when T_a goes continuously from T_c to T_p, M_j *remains unstable* and moves from M_c toward P (see Fig. 1), i.e., from case **1** to case **3b**. Also, N_j moves from N_c toward P, i.e., from case **5** to case **7**, passing through cases **6b** and **8** (see Eq. (31)). According to Table 2, if N_j represents case **6b** (or **8**) while M_j corresponds to case **1** (or **3a**) the situation leads naturally to a limit cycle (i.e., self-sustained oscillations).

Under conditions (16)–(18) the value of T_2 is approximately given by (use Eq. (52) with Eq. (48b))

$$T_2 \approx T_c\left(1 - \frac{T_c}{C''}\right) \quad (54)$$

which is very near T_c. Moreover, a *necessary condition* (i.e., the inverse of inequality (53)) to obtain self-sustained *oscillations* in this L–H case ($n = 1$) reads

$$T_c < \tfrac{1}{2}[RC_cC'']^{1/2}. \quad (55)$$

According to definition (23b), this condition (55) should be the most easily satisfied if A_T

is small as is the case with thin catalyst dots supported by a thermally resistant material (*18*).

B. Stability Analysis of the L–H Adsorbates: Case n = 2

If $n = 2$ (see Eq. (8)), besides the *pure* steady-state adsorbates (34) there exist *mixed* steady-state adsorbates (see Eqs. (35a)–(35c)) which correspond to a *pair* of *symmetric* points (see Fig. 2):

$$M_j^* \equiv [X_0 = \bar{X}_0(1 + \delta), \quad Y_0 = \bar{X}_0(1 - \delta), \ T_0], \tag{56a}$$

$$N_j^* \equiv [X_0 = \bar{X}_0(1 - \delta), \quad Y_0 = \bar{X}_0(1 + \delta), \ T_0], \tag{56b}$$

with

$$T_0 = T_a + RB_1^2/B_2, \tag{57}$$

where R is defined by Eq. (23b). Moreover

$$\bar{X}_0 = \tfrac{1}{2}(1 - B_1/B_2) \tag{58}$$

and δ is the positive square root of

$$\delta^2 = 1 - 4B_1^2B_2/(B_2 - B_1)^2C. \tag{59}$$

In Eqs. (57)–(59) B_1, B_2, and C are evaluated at T_0. Mixed adsorbates ((56a), (56b)) can only be obtained when

$$T_c < T_c^* < T_0, \tag{60}$$

where T_c is given in Eq. (37a) and T_c^* is defined by the relation $\delta = 0$. If

$$B_2'/B_1' > 1 + 2(B_2'/C')^{1/2}, \tag{61}$$

T_c^* is *unique* and approximately given by

$$T_c^* \approx (C'' + B_2'' - 2B_1'')/\ln(B_2'C/4B_1'^2). \tag{62}$$

Equations (57) and (60) define an *onset* ambient temperature T_p^* for mixed adsorbates (compare with case $n = 1$, Eqs. (42), (43)):

$$T_p^* \leq T_a, \tag{63}$$

$$T_p^* = T_c^* - RB_1^2/B_2|_{T_c^*}. \tag{64}$$

For $T_a = T_p^*$, solutions ((56a), (56b)) coincide at point $P^* = \{X_c^*, Y_c^*, T_c^*\}$, where $X_c^* = Y_c^* = \bar{X}_0(T_c^*)$ (see Fig. 2). When T_a increases away from T_p^*, the quantity δ (59) comes close to unity in a few degrees. Hence the curve corresponding to the mixed adsorbates in Fig. 2 is broad-open.

For the *pure* adsorbates (34) the Jacobian matrix A (24) has the three following eigenvalues:

$$\lambda_{1,2} = -\tfrac{1}{2}\{(B_1 + C) \pm [(B_1 + C)^2 - 4B_1C(X_0 - Y_0)]^{1/2}, \quad \lambda_3 = -A_T. \tag{65}$$

Therefore M is stable while N is unstable; the surface can never be entirely covered with reactant B (see Fig. 2).

For the mixed adsorbates ((56a), (56b)) the S_i's take the following approximate forms provided condition (16) is satisfied and $B_1'' \approx 0$:

$$S_1 \approx -3B_1, \tag{66a}$$

$$S_2 \approx 3A_TB_1 \mp 2B_1C\bar{X}_0\delta - B_1[(\beta_2 - \beta_1)B_2'' + (4\beta_2 + 2\beta_1 + 3\gamma)C''](T_0 - T_a)/RT_0^2, \tag{66b}$$

$$S_3 = \pm 2A_TB_1C\bar{X}_0\delta[1 + B_2''(T_0 - T_a)/T_0^2], \tag{66c}$$

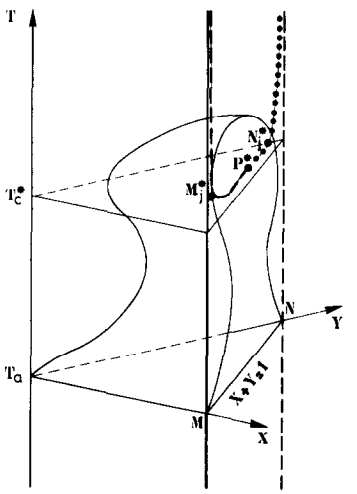

FIG. 2. Representation of the L–H steady-state lines and of the L–H heat surface in the case $n = 2$. The steady-state points M_j^* and N_j^* are defined in Eqs. (56a) and (56b).

where the upper (lower) sign refers to M_j^* (N_j^*). The stability characteristics of points M_j^* and N_j^* depend on the parameter ($T_0 - T_a$) which, contrary to the case $n = 1$ (see Eq. (50)), is *not* a free parameter. According to Eq. (57), ($T_0 - T_a$) is forced to retain an almost constant value:

$$T_0 - T_a \approx q_1/(1 + q_1 q_2) \qquad (67)$$

with

$$q_1 = RB_1^2/B_2|_{T_a},$$
$$q_2 = (B_2'' - 2B_1'')/T_a^2 < 1. \qquad (68)$$

Moreover, as $C'' > B_2''$ (see Eq. (18)), $S_2 > 0$ (see Eq. (66b)) if

$$T_0 - T_a \ll T_a^2/C''. \qquad (69)$$

According to Table 4, if condition (69) is satisfied, point M_j^* is *unstable* (case **1**) and N_j is *stable* (case **5**). If inequality (69) is reversed (i.e., $S_2 < 0$), M_j^* *remains unstable* while N_j^* *becomes unstable* (case **7**). When S_2 is not appreciably different from zero, i.e., if $C'' > B_2''$ when

$$q_1 \approx T_a^2/C'', \qquad (70)$$

N_j^* can represent case **6a** (or **8**) while M_j^* represents case **1** (or **3a**). According to Table 2, this situation could lead to limit cycles.

5. "ELEY-RIDEAL" CASE

In this case the L–H mechanism (step 3 in Table 1) is neglected, i.e.,

$$C = 0. \qquad (71)$$

Under this condition, the E–R steady states $\{X_0, Y_0, T_0\}$ may be visualized in the phase space as the intersection points of the E–R steady-state *line* $\{X_0(T), Y_0(T)\}$ obtained from Eqs. (20a) and (20b), i.e.,

$$A_1X_0 - B_1(1 - X_0 - Y_0) = 0, \qquad (72a)$$

$$x_0^n = \left(\frac{B_1}{A_1}\right)^n \left(\frac{A_2}{B_2}\right) Y_0 (n = 1, 2), \qquad (72b)$$

with the E–R *heat plane* (see Eqs. (21)–(23a)):

$$T - T_a \approx LA_2Y, \quad (\alpha_1 \approx -\beta_1,\ n = 1, 2). \qquad (73)$$

At a *fixed* surface temperature, say T, the mixed E–R adsorbate is represented by the intersection point I (always in the phase space triangle at T) of the lines ((72a), (72b)). The straight line (72a) (represented by the heavy line in Figs. 3A, B) crosses the Y-axis at point N ($X = 0$, $Y = 1$) and the X-axis at the A-"Langmuir isotherm" coordinate X_L (see Eq. (19)) which moves toward zero when T increases. The second line (72b) (represented by the dashed line in Figs. 3A, B),

$$X_0 = a(T)Y_0,\ a(T) = \left(\frac{B_1}{A_1}\right)\left(\frac{A_2}{B_2}\right), \quad n = 1, \qquad (74)$$

$$X_0^2 = b(T)Y_0,\ b(T) = \left(\frac{B_1}{A_1}\right)^2\left(\frac{A_2}{B_2}\right), \quad n = 2, \qquad (75)$$

passes through the origin and rotates from the X-axis toward the Y-axis when T increases since $a(T)$ and $b(T)$ decrease when T increases (see Eq. (17)).

The E–R steady-state line therefore has the form of a spiral (confined in the prismatic phase space) such as is represented in Figs. 5A, B, which also show the E–R heat plane (73).

A. *Stability Analysis of the E–R Adsorbates: Case n = 1*

The solutions $\{X_0(T), Y_0(T)\}$ of Eqs. (72a) and (72b) have the form of the Langmuir isotherms for a *binary* mixture (*15*) as the E–R contribution A_2Y is formally equivalent to any molecular desorption term. According to condition (16) we have for n = 1:

$$X_0 = \frac{B_1/A_1}{1 + B_1/A_1 + B_2/A_2} \approx a(1 + a)^{-1}, \qquad (76a)$$

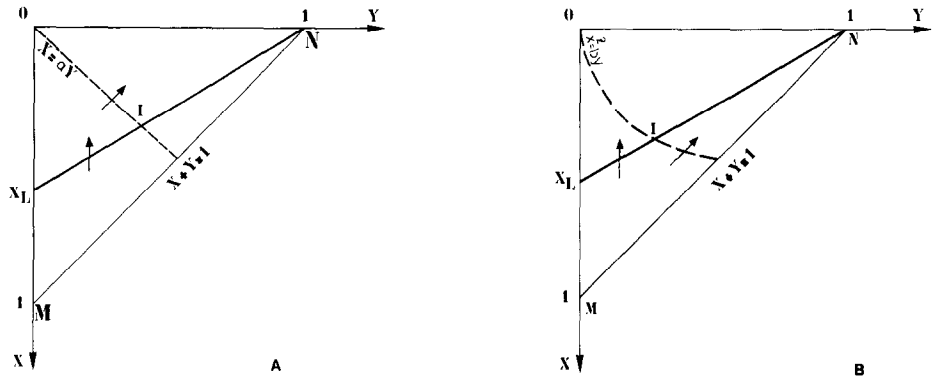

FIG. 3. (A) Representation in a T-fixed plane of Eq. (72a) (Eq. (72b), case $n = 1$) by the solid (dashed) line. Both lines intersect at point I. When T increases the lines move according to the arrows and intersection point I moves from M toward N (see the E–R steady-state line in Figs. 5A, B). Representation in a T-fixed plane of Eq. (72a) (Eq. (72b), case $n = 2$) by the solid (dashed) line. Both lines intersect at point I. When T increases the lines move according to the arrows and intersection point I moves from M toward N. The steady-state line in this case $n = 2$ is analogous to that of the case $n = 1$ (see Figs. 5A, B).

$$Y_0 = \frac{B_2/A_2}{1 + B_1/A_1 + B_2/A_2} \approx (1 + a)^{-1}, \quad (76b)$$

where $a(T)$, defined in Eq. (74), has to be evaluated at T_0. This steady-state temperature T_0 is implicitly defined by the heat equation (see Eq. (73)):

$$T_0 - T_a \approx g \equiv LA_2Y_0, \quad (77)$$

where L is given in Eq. (23a). For a given value of T_a, Eq. (77) admits in practice one or three solutions. Figure 4 shows that if, *at the inflection point* of $g(T)$, its slope g' is less than unity ($g_i' < 1$), *any* steady-state temperature T_0 is *unique*. Using the approximate form (see Eqs. (16) and (17))

$$g' \approx g\frac{(A_1'' + B_2'')}{T^2}(1 - Y) \quad (78)$$

obtained from Eqs. (76) and (77) we can explicitly specify the necessary condition

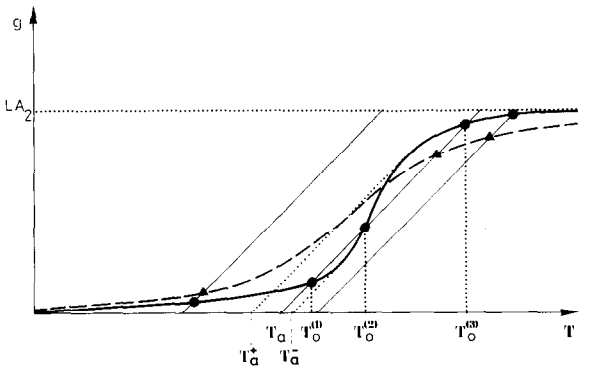

FIG. 4. Graphical resolution of the steady-state temperature equation (77). When the slope $g_i' > 1$ (see heavy line) three E–R steady states are possible for $T_a^+ < T_a < T_a^-$ (see Fig. 5A). If $g_i' < 1$ (dashed line) only a unique E–R steady state occurs. This figure concerns case $n = 1$ as well as case $n = 2$.

to obtain one *unique* E–R steady state as:

$$\frac{LA_2}{(A_1'' + B_2'')} < \tfrac{1}{2}\left\{\left[1 + \left(\frac{4T_s}{A_1'' + B_2''}\right)^2\right]^{1/2} - 1\right\}, \quad (79)$$

where T_s is the "stoichiometric temperature" defined by $a\ (T_s) = 1$ (see Eq. (74)), i.e., with $a_\infty \equiv a(T = \infty)$,

$$T_s = -(A_1'' + B_2'')/\ln a_\infty. \quad (80)$$

One realizes from Fig. 4 that if $g_i' > 1$, i.e., if the inequality *opposite* to Eq. (79) is verified, one obtains the following situations depending on the value of T_a:

(i) for $T_a < T_a^+$, there exists one single steady state which is stable (see after Eq. (81c) below);

(ii) if $T_a^+ < T_a < T_a^-$, there exist always three steady states, one of them (i.e., the steady state corresponding to $T_0 \gtrsim T_a$, e.g., $T_0^{(1)}$ in Fig. 4) being stable (see below);

(iii) for $T_a^- < T_a$, a single (stable or unstable) steady state occurs. The temperatures $T_a^\pm$ may be computed from Eq. (77) for $T_0^\pm$ and for $T_0 = T_s$ using the values $Y_0^\pm$ obtained from the evident relation $g'\ (T_0 = T_0^\pm) = 1$. Figures 5A and B illustrate how the E–R steady-state line $\{X_0(T),\ Y_0(T)\}$ crosses the E–R heat plane (73).

Provided condition (16) is satisfied and $A_2'' \approx B_1'' \approx 0$, the S_i's for the E–R steady states ((76), (77)) may be cast into

$$S_1 \approx -(B_1 + B_2), \quad (81a)$$

$$S_2 \approx A_T(B_1 + B_2) + (A_1B_2 + A_2B_1) - A_TB_1\frac{(\beta_2 - \beta_1)}{(\beta_2 - \alpha_2)} (A_1'' + B_2'')(T_0 - T_a)T_0^{-2}, \quad (81b)$$

$$S_3 \approx -A_T[(A_1B_2 + A_2B_1) - A_2B_1(A_1'' + B_2'')(T_0 - T_a)T_0^{-2}]. \quad (81c)$$

These definitions show that any steady state with $T_0 \gtrsim T_a$ (e.g., $T_0^{(1)}$ in Fig. 5) is *stable* (case 5 in Table 2). Such a stable case appears when inequality (79) is reversed *and* $T_a < T_a^-$ (see cases (i) and (ii) above). To go further with the stability analysis let us concentrate on *unique* steady states. We first rewrite S_2 and S_3, Eqs. (81b) and (81c),

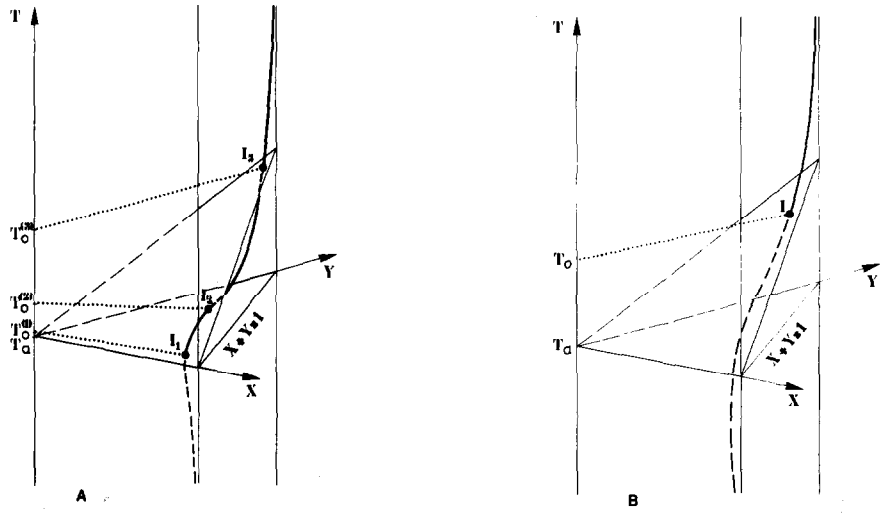

FIG. 5. (A) Representation of the E–R steady-state line and the E–R heat triangle (73) for three steady-state points I_1, I_2, I_3 (see heavy line in Fig. 4). The steady-state I_1 (with $T_0 = T_0^{(1)} \gtrsim T_a$) is stable (see text). This figure concerns case $n = 1$ as well as case $n = 2$. (B) Representation of the E–R steady-state line and the E–R heat triangle (73) for a unique steady-state point (see dashed line in Fig. 4). This figure concerns case $n = 1$ as well as case $n = 2$.

as

$$S_2 \approx A_T(B_1 + B_2) + (A_1B_2 + A_2B_1)(1 - \frac{\beta_2 - \beta_1}{LA_2} g') \equiv A_T(B_1 + B_2)(1 - L/L_2) \quad (82a)$$

$$S_3 \approx A_T(A_1B_2 + A_2B_1)(L/L_3 - 1), \quad (82b)$$

with

$$L_3 \equiv L/g', \qquad L_2 > FL_3, \quad (83)$$

where g' is given in Eq. (78) and F is defined in Eq. (85) below. According to Table 3, *sustained oscillations*, i.e., case **6b** (or **8**) of Table 2, require $S_2 \gtrsim 0$ (or $S_2 \lesssim 0$) with $S_3 < 0$, i.e., $g' < 1$. We can thus deduce from Eqs. (82a) and (82b) two *necessary* conditions for oscillations, i.e., for a given value of L (see Eq. (23a)):

$$\frac{A_2(\beta_2 + \alpha_2)}{A_T(\beta_2 - \beta_1)} < g' < 1 \quad (84)$$

and

$$F \equiv \frac{(1 + A_2Y_0/A_1X_0)(\beta_2 + \alpha_2)}{(1 + Y_0/X_0)(\beta_2 - \beta_1)} < 1. \quad (85)$$

These conditions imply respectively

$$A_T > A_2 \qquad \text{and} \qquad A_1 > A_2. \quad (86)$$

On the contrary, if with condition (84) still satisfied

$$A_T > A_2 \qquad \text{and} \qquad A_2 > A_1, \quad (87)$$

one has $F > 1$ and the steady state is stable (case **5** of Table 2).

It should be added that the second inequality in Eq. (86) implies that, under condition (16), an oscillatory pure E–R reaction could occur only if the E–R "cross section" σ_{E-R} (of step 4 in Table 1) is smaller than the sticking probability for gas A (i.e., $\sigma_{E-R} < \sigma_A$, see Eq. (11)).

B. Stability Analysis of the E–R Adsorbates: Case n = 2

In this case $n = 2$ the E–R steady states $\{X_0, Y_0, T_0\}$ are given by

$$X_0 = -\frac{kb}{2}[1 - (1 + 4/k^2b)^{1/2}], \quad (88a)$$

$$Y_0 = 1 - kX_0, \quad (88b)$$

with

$$k = 1 + A_1/B_1 \approx 1 \quad (89)$$

and b (given in Eq. (75)) evaluated at T_0 defined by Eq. (77). The heat equation being the same as for $n = 1$ and the steady-state line $\{X_0(T), Y_0(T)\}$ analogous for both values of n we can refer to Figs. 4 and 5 for the geometry analysis. Also the stability analysis follows here the same lines as above.

For a given value of T_a we have a unique E–R steady state provided $g_i' < 1$ (see below Eq. (77)). Using the relation

$$g' \approx g\frac{(2A_1'' + B_2'')}{T^2} \cdot \frac{(1 - Y)}{(1 + Y)} \quad (90)$$

obtained from Eqs. (88a) and (88b) with $k = 1$ and setting $A_2'' = B_1'' = 0$ we can specify this necessary condition for a unique E–R steady state. Under condition (16) the result reads:

$$(2A_1'' + B_2'')/T_i < (6T_i/LA_2). \quad (91)$$

The "inflection temperature" T_i is defined as

$$T_i = T_s^*/[1 + LA_2/2(2A_1'' + B_2'')] < T_s^* \quad (92)$$

with respect to the "stoichiometric temperature" which T_s^* corresponds to $b(T_s^*) = 1/2$ (see Eq. (75)), i.e., with $b_\infty \equiv b(T = \infty)$.

$$T_s^* = -(2A_1'' + B_2'')/\ln b_\infty. \quad (93)$$

Here again, if the inequality (91) is reversed *and* $T_a < T_a^-$ (see Fig. 5A), there exists always one *stable* steady state and sustained oscillations are forbidden.

Let us investigate the single steady states which occur when condition (91) holds *or* when this inequality (91) is reversed with $T_a > T_a^-$ [see case (iii) under Eq. (80) for analogy]. Following the same procedure as

for $n = 1$, we may show from the S_i's (under condition (16) and for $A_1'' \approx B_1'' \approx 0$) that the two *necessary* conditions for oscillations are again Eqs. (84) and (85) with, in this case $n = 2$,

$$F \equiv \frac{(1 + 2A_2Y_0/A_1X_0)(\beta_2 + \alpha_2)}{(1 + 2Y_0/X_0)(\beta_2 - \beta_1)}. \quad (94)$$

Therefore, if condition (86) is satisfied, oscillations can occur, while if condition (87) is satisfied, the E–R steady state is stable.

6. GENERAL CASE AND CONCLUSIONS

Rather than go into the complicated algebraic analysis for the general equations ((14a)–(14c)) under prescription (16) let us infer some geometrical arguments using the results of Sections 4 and 5. Most of the arguments sketched below have been checked numerically (e.g. (*11*)).

In the two-reaction-path model the steady-state line is a simple deformation of the E–R steady-state line (see Fig. 6). Due to the activated L–H contribution ($\sim CX_0Y_0$) the steady-state line becomes more bent in its central part than in the E–R case. In the relevant temperature range the variation of the coverage ratio $\Delta(X_0/Y_0)$ for a given variation ΔT increases when C increases with respect to the A_i's ($i = 1, 2$). In Fig. 6 the rounding toward $M(N)$ is a measure of the ratio A_1/C (A_2/C).

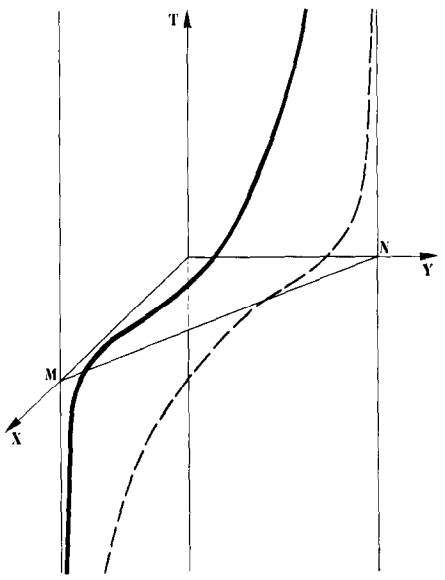

FIG. 6. Steady-state lines for the general case, i.e., when both L–H and E–R mechanisms are involved in the model. The rounding toward M (N) is a measure of the ratio A_1/C (A_2/C). The heavy (dotted) line corresponds to the general case with $A_2 \gg A_1$ ($A_2 \ll A_1$).

The general approximate heat surface (22) is a simple deformation of the L–H heat surface which, when completed by the E–R contribution ($\sim A_2Y$), partly loses its X–Y symmetry.

As it appears that the E–R mechanism stabilizes the reaction (see Eq. (87)) while the L–H mechanism leads easily to instabilities once it is activated (see Eq. (55) for instance) we conclude that within the general model the most favorable case for instabilities is such that

$$(B_2, B_1) > C > A_2 \approx A_1. \quad (95)$$

This conclusion has been illustrated by simulating sustained oscillations in the case of the CO oxidation on Pt (*11*).

The number of intersection points of the steady-state line with the heat surface *is always odd* (practically one or three, see Figs. 7A, B). The steady-state temperature equation

$$T_0 - T_a = g \equiv LA_2Y_0 + RCX_0Y_0 \quad (\alpha_1 = \beta_1) \quad (96)$$

can be analyzed along the same lines of the E–R case (see Section 5A). The crucial condition $g'(T_0) < 1$ characteristic of a unique steady state for a given value of T_a may be satisfied. As seen on Figs. 7A, B, in this case the points I_1 and I_2 come closer together and the steady-state line may eventually miss the surface temperature in the region $T_0 \gtrsim T_a$, leaving only a single steady state represented by I_3 (usually in the coverage regime $Y_0 > X_0$).

The stability analysis of such a unique steady state leads to a local behavior that corresponds to one of the cases reported in the lower part of Table 3. The passage from case 5 to case 7 according to sequence (31) is made possible by increasing the

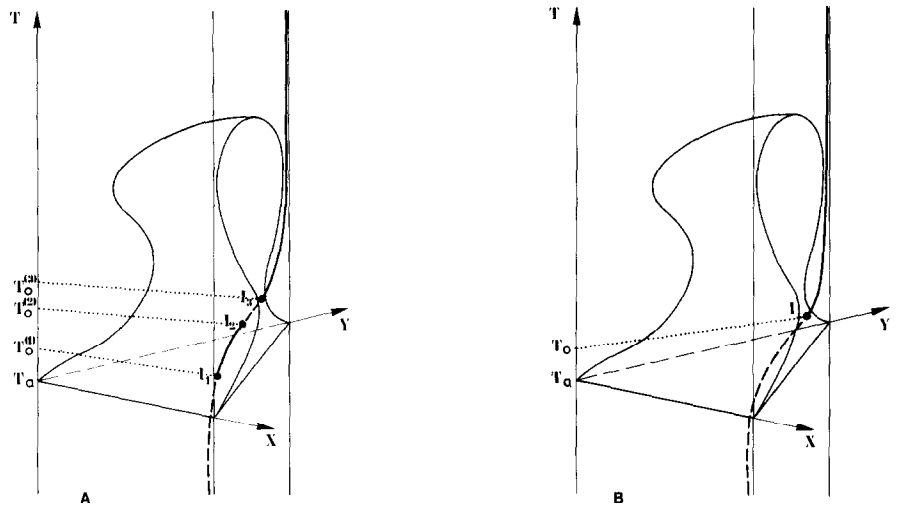

FIG. 7. (A) Representation of the steady-state line and of the heat surface in the general case for three steady-state points I_1, I_2, I_3. The steady state I_1 (with $T_0 = T_0^{(1)} \gtrsim T_a$) is stable. (B) Representation of the steady-state line and of the heat surface in the general case for a unique steady-state point.

coefficients L and R (i.e., essentially by *lowering* the "dissipative factor" A_T, see Eqs. (23a) and (23b)), all the "chemical" parameters A, B, C satisfying condition (95). The steady states corresponding to case **6b** or **8** (i.e., sustained oscillations) occur for $Y_0 > X_0$, i.e., for $T_0 - T_a$ of the order of 10–20° (e.g., (*11*)).

It results from our analysis that oscillations could be observed in bimolecular surface reactions provided that:

(1) The ambient temperature T_a is adjusted about T_c^* within a margin of a few degrees (see Eq. (95)). The adsorption of one reactant must be activated (i.e., dissociative). In this case, Eq. (62) could be used to approach T_c^*.

(2) A highly activated L–H mechanism is involved in the reaction scheme. This is in order to observe high-frequency oscillations with significant variations of the adsorbate composition (e.g., (*11*)).

(3) The experimental setup is made of *small* catalyst pellets or dots supported by a *thermally resistant* material. This is to allow for the surface temperature to depart coherently from $T_a \approx T_c^*$.

One should finally mention the main drawback of this model: significant variations of the adsorbate composition need rather large variations of the surface temperature T (e.g., a variation $\Delta Y \approx + 0.1$ requires a jump $\Delta T \approx$ 30–40° (*11*)). The introduction in thermochemical-surface-oscillation models of "isothermal" ingredients like coverage-dependent activation energies (e.g., an L–H activation energy C'' decreasing when $y = \theta_B$ increases) should remedy this situation. Further work in this direction is underway. Experimental evidence of activation energies depending on *specific* coverages would be welcome. The presence of temperature oscillations is the main conclusion which can be drawn from our model. We therefore would like to ask experimentalists to try to devise methods to measure the surface temperature (i.e., the temperature of the first few layers) of the catalyst in a very precise way during the reaction. In our view, the mere existence of a significant difference between the bulk temperature and the surface temperature would in itself be a major progress in the field.

REFERENCES

1. Fieguth, P., and Wicke, E., *Chem. Ing. Tech.* **43,** 64 (1971).
2. Beusch, H., Fieguth, P., and Wicke, E., *Chem. Ing. Tech.* **44,** 445 (1972).
3. Dauchot, J. P., and Van Cakenberghe, J., *Nature (London) Phys. Sci.* **246,** 61 (1973); *Japan. J. Appl. Phys. Suppl.* **2**(2), 533 (1973).
4. McCarthy, E., Zahradnik, J., Kuczynski, G. C., and Carberry, J. J., *J. Catal.* **39,** 29 (1975).
5. Plichta, R. T., thesis, University of Illinois, Urbana, 1976.
6. Nitta, M., Kanefusa, S., Taketa, Y., and Haradome, M., *Appl. Phys. Lett.* **32,** 590 (1978).
7. Belyaev, V. D., Slin'ko, M. M., Slin'ko, M. G., and Timoshenko, V. I., *Kinet. Katal.* **14,** 810 (1973); *Dokl. Akad. Nauk SSSR* **214,** 1098 (1974).
8. Barelko, V. V., and Volodin, U. E., *Dokl. Akad. Nauk SSSR* **211,** 1373 (1973); **216,** 1080 (1974); *Kinet. Katal.* **17,** 683 (1976).
9. Schwartz, A., Holbrook, L., and Wise, J., *J. Catal.* **21,** 199 (1971).
10. Al'tshuller, O. V., *et al., in* "Transactions of the All-Union Conference on Heterogeneous Catalytical Reaction Mechanisms." IKhF AN SSSR Press, Moscow, 1974 (Preprint 77).
11. Dagonnier, R., and Nuyts, J., *J. Chem. Phys.* **65,** 2061 (1976).
12. To our knowledge, surface reaction oscillations *at low pressure* have not been reported up to now.
13. Slin'ko, M. G., and Slin'ko, M. M., *Catal. Rev. Sci. Eng.* **17,** 119 (1978).
14. Hayward, D. O., and Trapnell, B. M. W., "Chemisorption." Butterworths, London, 1964.
15. Clark, A., "The Theory of Adsorption and Catalysis." Academic Press, New York, 1970.
16. Bond, G. C., "Catalysis by Metals." Academic Press, New York, 1962.
17. Bonzel, H. P., and Burton, J. J., *Surface Sci.* **52,** 223 (1975).
18. Steinbrüchel, Ch., and Schmidt, L. D., *Surface Sci.* **40,** 693 (1973).
19. See for instance, Sattinger, D. H., "Topics in Stability and Bifurcation Theory." Springer-Verlag, Berlin, 1973.
20. Reyn, J. W., *Z. Angew. Math. Phys.* **15,** 540 (1964).
21. Nicolis, G., and Prigogine, I., "Self-organisation in Non-equilibrium Systems." Wiley–Interscience, New York, 1977.
22. Attenuation of the oscillations conjugated with an increase of their frequency has been observed in Pt-catalyzed CO oxidation by using supports with high thermal conductivity (e.g., NaCl) and/or by mixing the active gases with He (high thermal conductivity) (J. Van Cakenberghe, private communication).